Journal of Applied Polymer Science

Crystal violet dye sorption and transport in/through biobased PVA cryogel membranes

Adina Papancea, Silvia Patachia, Rodica Dobritoiu
Department of Product Design, Mechatronics and Environment, Transilvania University of Brasov, Brasov 500036, Romania
Correspondence to: S. Patachia (E-mail: st.patachia@unitbv.ro)

ABSTRACT: Cryogels based on poly(vinyl alcohol) [PVA] and three types of bioinsertions such as scleroglucan, cellulose microfibers, and zein, respectively, have been prepared using capacity of PVA to crosslink by repeated freezing–thawing cycles. The effect of the incorporation of biopolymers on the properties of PVA cryogel has been studied by using several techniques such as: scanning electron microscopy, differential scanning calorimetry, and Fourier transform infrared studies. The obtained biobased cryogel membranes were subjected to sorption and to diffusion experiments using Crystal Violet (CV), a dye commonly used in the textile industry and in medicine. Image analysis with CIELAB system was used both to monitor the cryogels loading with CV and to gain insight in the dye state into the gel, in correlation with the bioinsertion type and gels morphology. Dye diffusion but also sorption capacity of the cryogels was found to be closely related to the type of biopolymer. In this article the equilibrium (sorption isotherms) and transport properties (diffusion and permeability coefficients) of CV, in/through physical cross-linked PVA hydrogel membranes with bioinsertions has been reported. The highest efficiency for the CV removal from aqueous solutions was obtained for the PVA/Scl cryogels.
 J. Appl. Polym. Sci. **2015**, *132*, 41838.

KEYWORDS: biopolymers; characterization; crystal violet; gels; membranes; PVA; sorption

Received 20 August 2014; accepted 3 December 2014
DOI: 10.1002/app.41838

INTRODUCTION

Nowadays, due to the environmental policy constraints, researchers are looking for ecological substrates for dyes sorption from aqueous solutions.[1–6] In these conditions, due to its properties (water solubility, non-toxicity, non-carcinogenity, biodegradability, biocompatibility, capacity to form gels by cryogenic techniques[7–9]), poly(vinyl alcohol) (PVA) is a proper candidate who has the capacity to be blend with other polymers or to be matrix for different fillers allowing obtaining of new materials with controlled properties.[10,11] Due to the ease of obtaining, to their special sorption and transport properties, the PVA cryogels were studied in different contexts both for retention of metal ions,[12] dyes,[13] or ionic liquids.[14,15] The mentioned biobased cryogels gave good results also for Methylene Blue sorption (MB).[11]

The aim of this work is to extend and compare the sorption studies in PVA biobased cryogels for different types of dyes [Crystal Violet (CV) and MB] that could be find both, singular, or simultaneous, in waste waters as pollutants, and also loaded into gels, as systems for disinfectants controlled release or in antimicrobial colored fibers. Another aim is to gain insight in the influence of the dye molecular structure on its thermodynamic and kinetic sorption and diffusion in/from/through the studied cryogels as well as into the state of dye into the gel matrix that influences the gels color.

The natural polymers used like bioinsertions were: scleroglucan (Scl), microfibers of cellulose (Cel), and zein. Scl, a natural polysaccharide, produced by fungi of Sclerotium type, has a stable triple-stranded helical conformation held together by hydrogen bonds. Its helical structure plays an important role in determining the mechanism of sorption outside and inside of the helix.[13,14,16] Cel have higher specific surface area compared with other conventional cellulose fibers and could act like a reinforcement for polymers due to the removal of amorphous regions by acid hydrolysis.[17,18] Zein, a prolamine which comprises about 45%–50% of corn protein content,[19] has good potential to interact with other compounds due to amino or carboxyl groups present in its structure. CV, a cationic dye and antimicrobial agent, was used to evaluate the capacity of cryogels to be loaded with this dye and to remove it from aqueous solutions.

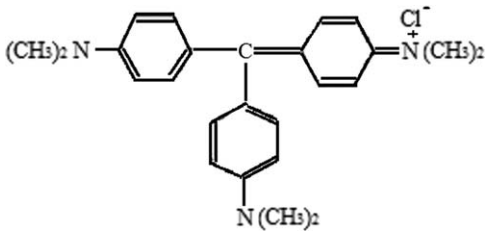

Figure 1. Structure of CV.

EXPERIMENTAL

Materials

- PVA 98%–99% was hydrolyzed ($M = 146{,}000$–$186{,}000$) from Sigma-Aldrich.
- Biopolymers: Scl (Actigum CS 11, $M_w = 1{,}000{,}000$ Da) was obtained from Cargill, St-Germain-en-Laye, France; and Zein was obtained from Sigma-Aldrich. The polymers were used without further purification. Microfibers of cellulose were prepared as follows: a dispersion of cellulose microfibers was obtained by hydrolysis of cotton wool in HCl medium, procedure adapted from a method described by Kim *et al.*[20] After hydrolysis, the suspension was diluted with distilled water and then allowed to settle and subsequently was washed until pH became neutral [the solid content (SC) of the dispersion was 36.2%].
- CV purchased from Fluka was used as received without further purification. In Figure 1, the structure of CV is presented. Solutions of CV at desired concentrations (1×10^{-6}, 3×10^{-6}, 5×10^{-6}, and 7×10^{-6}, 1×10^{-5} mol/L) were prepared by using distilled water. The concentration range considered was selected taking into account the solubility of dye in water (16 g/L).[21]

Preparation of PVA and PVA/Natural Polymers Cryogels

The solutions of PVA and Scl, have been prepared according to the method described by Patachia *et al.*[20] PVA, PVA/Scl, PVA/Cel, and PVA/Zein hydrogels (cryogels) have been prepared as described by Dobritoiu and Patachia.[11] Briefly, a PVA solution of 10 wt % concentration was prepared by dissolving a certain amount of PVA into distilled water at 90°C under continuous stirring for 3 hours. PVA/Scl hydrogels (cryogels) have been prepared by mixing solutions of PVA (10%) and Scl (1%) for a few minutes in a beaker and then pouring them in a PVC cylindrical recipient. To obtain PVA/Cel cryogel, the dispersion of Cel (SC by 36.2%) has been mixed with PVA solution (10%) (in 9 : 1 weight ratio of polymers) under continuous stirring for 1 h. To prepare PVA/zein cryogel, zein powder was dispersed into a PVA/water/DMSO solution (prepared by adding the corresponding PVA powder to a mixture of water and DMSO, in a weight ratio of 1 : 4, followed by heating at 90°C and continuous stirring, for 2 hours) under continuous stirring for 1 h. The polymers weight ratio was 9 : 1. After mixing the solution, it was cast in Petri dishes and submitted to freezing for 12 h at −20°C and, after that, it was thawed for 12 h at +25°C. The cycles of freezing and thawing were repeated three times. To improve flexibility and mechanical strength of cryogels each one was immersed in KOH 4*M* solution for 30 min, a procedure adapted from Fu *et al.*[22] The adsorbed KOH on the surface of the cryogel was removed by rinsing it in distilled water several times, until neutral pH. Then the cryogels were stored in distilled water for later use.

Methods for Cryogels Characterization

SC and Swelling Degree (SD) of the Cryogels. The obtained cryogels were cut into round pieces of about 0.5–1.5 g and 0.2–0.3 mm thickness. The SC of the cryogels, as they resulted after the preparation, has been determined gravimetrically and calculated by using eq. (1).

$$\text{SC}\ (\%) = \frac{m_{\text{xerogel}}}{m_0} \times 100 \quad (1)$$

where, m_{xerogel} is the mass of the dried cryogel, immediately after it's preparation and m_0 is the initial mass of the cryogel after preparation.

The obtained cryogels were then conditioned by immersing in distilled water, aiming to reach the swelling equilibrium. The SD was calculated with eq. (2).

$$\text{SD}\ (\%) = \frac{m_e}{m_{\text{xerogel}}} \times 100 \quad (2)$$

where, m_e is the mass of the swollen sample, balanced in water, and m_{xerogel} is the mass of dried sample.

Differential Scanning Calorimetry (DSC). The crystalline structure of the membranes was investigated by DSC using a Diamond DSC Heat Flow Perkin Elmer with a heating rate of 5°C/min, from 20°C to 250°C and then cooled with the same rate for three cycles. The membranes were air-dried, and then submitted to DSC analysis. The crystallinity degree (CD) was calculated as the ratio between the enthalpy of fusion (ΔH_f) of the PVA or PVA with bioinsertions and the enthalpy of fusion of PVA in its completely crystalline state (H°_f)[23] which for PVA is 138.6 J/g.[24]

Scanning Electron Microscopy (SEM). The surface morphology of PVA membranes was analyzed by SEM with a Hitachi-3500N, scanning microscope operating under low vacuum at 20 kV. The samples were dried in air for 10 days and then analyzed without further preparation by placing them on a holder using a carbon double-sided conductive tape.

Fourier Transform Infrared (FTIR) Spectroscopy. The FTIR spectra analysis has been performed by using a FTIR spectrometer (Perkin Elmer BXII) working in Attenuated Total Reflectance mode, with a total of four scans with a 2 cm^{-1} resolution, within a spectral range of 4000–600 cm^{-1}. Dried samples of each cryogel were analyzed on three different samples.

CIELAB Analyses. The change in biobased cryogels color and in aspect, after CV sorption, was analyzed through CIEL*a*b* system (CIELAB). This method gives important information concerning the concentration of the dye into the gel, the aggregation state of the dye, and its distribution into the gel mass. CIELAB gives the possibility to make difference between two very close colors by taking into account parameters such as: hue, saturation, and luminosity. The CIELAB color space parameters are: L^*, color luminosity, varies from 100 (white) to 0 (black); a^* varies from red ($+a^*$) to green ($-a^*$) and b^*

varies from yellow ($+b^*$) to blue ($-b^*$). Using differences in a^*, b^*, and L^* parameters [eq. (3)] the difference in color (ΔE^*_{ab}) was calculated [eq. (4)].

$$\Delta X = X_1 - X_0 \tag{3}$$

where X is one of the color coefficients L^*, a^*, or b^*, whereas 1 and 0 indices, are the initial value for the cryogel dye loaded sample and the value for the cryogel sample immersed in solution with lowest concentration (c_1)

$$\Delta E^*_{ab} = \sqrt{\Delta L^{*2} + \Delta a^{*2} + \Delta b^{*2}} \tag{4}$$

Sorption Studies. Samples with masses between 0.1 and 0.3 g were immersed in CV solutions in the following concentrations: $c_1 = 1 \times 10^{-6}$, $c_2 = 3 \times 10^{-6}$, $c_3 = 5 \times 10^{-6}$, $c_4 = 7 \times 10^{-6}$, $c_5 = 1 \times 10^{-5}$ mol/L. The sorption of CV was monitored through the analysis of the immersion solutions at different periods of time after the sample immersion. The change in solution absorbance was monitored using an ultraviolet–visible (UV/VIS) Perkin Elmer spectrophotometer, Lambda 25-model ($\lambda_{CV} = 590$ nm). The sorption equilibrium was reached after 20 days. The experiments were made at room temperature. The mass of the CV sorbed by cryogels was calculated by monitoring the concentration of the CV dye solutions as a function of time. The amount of CV adsorbed by the weight unit of cryogels, q_t (mg/g), was calculated with eq. (5):

$$q_t = \frac{(c_0 - c_t) \times M \times V}{m_{\text{xerogel}} \times 100} \tag{5}$$

where: c_0 (mol/L) and c_t (mol/L) are the solutions concentration at time $t = 0$ and at equilibrium time t, respectively; M is the molar mass of CV; V (L) is the volume of CV solution, and m_{xerogel} (g) is the mass of dried gel.

Diffusion Studies. The diffusion experiments have been carried out as follows: the diffusion cell has two compartments with a volume V of 250 mL, **A** the donor compartment and **B** the receptor compartment, interconnected through an opening of 0.659 cm^2 area (A). The membrane, with a thickness t_m, previously balanced in water, was placed between the two compartments. The diffusion cell was placed under a magnetic stirrer F20 FALC that ensures solutions homogenization in both compartments. To determine the amount of diffused dye that permeates the membrane, every 4 min, 4 mL of sample were extracted from B compartment. The solutions were analyzed using visible absorption spectroscopy on a UV–VIS Jasco V-530 at $\lambda_{CV} = 590$ nm, where the molar extinction coefficient is $\varepsilon = 87.000 M^{-1}$ cm^{-1},[25] on the basis of these measurements, the flux of dyes through the studied membranes was determined.[13] On the basis of these measurements, the integral diffusion, D_θ, and the permeation, P, coefficients were calculated[26] by the following equations:

$$D_\theta = \frac{t_m^2}{6\theta} \tag{6}$$

$$P = \frac{V t_m}{A c_i} \frac{dc}{dt} \tag{7}$$

where θ is the time-lag, t is the time, V is the volume of one compartment of the diffusion cell, A is the area of the opening between the two compartments of the diffusion cell, dc/dt is the dye permeation rate, and c_i is the initial concentration of the dye in solution in the compartment **A** of the diffusion cell.

Table I. SC (%), SD (%), and CD (%) for PVA and PVA Bioinsertion Cryogels

Cryogel composition	SC (%)	*SD* (%)	CD (%)
PVA	6.75	1481.48	38.03
PVA/Scl	4.08	2450.98	35.47
PVA/Cel	8.26	1210.65	28.46
PVA/Zein	14.86	672.95	25.48

RESULTS AND DISCUSSION

Using the obtained values for the SC (Table I) it can be observed that cryogels with low initial SC were highly swollen in balanced state. In case of PVA/Scl cryogels, the SC is the lowest, due to the low solubility of Scl in water and due to the necessity to maintain the same ratio between polymers, with the aim to compare their properties.

The effect of bioinsertions on the PVA CD is shown in Table I. CD has been calculated based on DSC thermograms presented in Figure 2. It is possible to conclude that in all cases, the bioinsertions are decreasing the CD of the PVA. A possible explanation for such behavior is that the presence of biopolymer in the PVA solution led to hindering the PVA–PVA interaction and as consequence to lowering of PVA crystallization.

The effect of bioinsertion on the surface morphology of the PVA-based gels was analyzed by SEM (Figure 3).

In SEM pictures it can observe that the pores dimension is decreasing in all cases comparing to the PVA cryogel. Also, organized, parallel structures are observed in the PVA/Scl cryogel and specific cellulose microfibers structures in the PVA/Cel cryogels. The incorporation of Zein into the PVA gel leads to a significant decrease in the surface porosity, suggesting a higher gel compaction as it follows: PVA/Scl > PVA/Cel > PVA/Zein, the same order shown by the CD decrease, in Table I. Analysis of PVA and PVA/biobased cryogels structure by FTIR spectroscopy revealed some alteration of the absorption bands intensity and bands shifting, meaning interaction between the components (Figure 4). So in Figure 4 one can observe a blue shift: from 3266.06 cm^{-1} for PVA to 3272.97 and 3273.87 cm^{-1}, respectively, in case of PVA/Zein and PVA/Cel, for the bands corresponding to O—H stretching vibration. This shift meaning could be disruption of H bonding between PVA macromolecules and this is in agreement with the CD decrease. In case of PVA/Scl cryogel, the shift of this band is from 3266.06 cm^{-1} for PVA to 3262.14 cm^{-1}, meaning formation of new H bondings. The decrease of the PVA/Scl CD suggests that the new H bonds were born by interaction between —OH groups both from PVA and from Scl. This is in close agreement with DSC analysis and with the shifted bands corresponding to skeletal vibration, from 843.05 and from 674.81 cm^{-1} for the PVA cryogels to 839.88 cm^{-1} and to 670.1 cm^{-1} for the PVA/Scl cryogels that

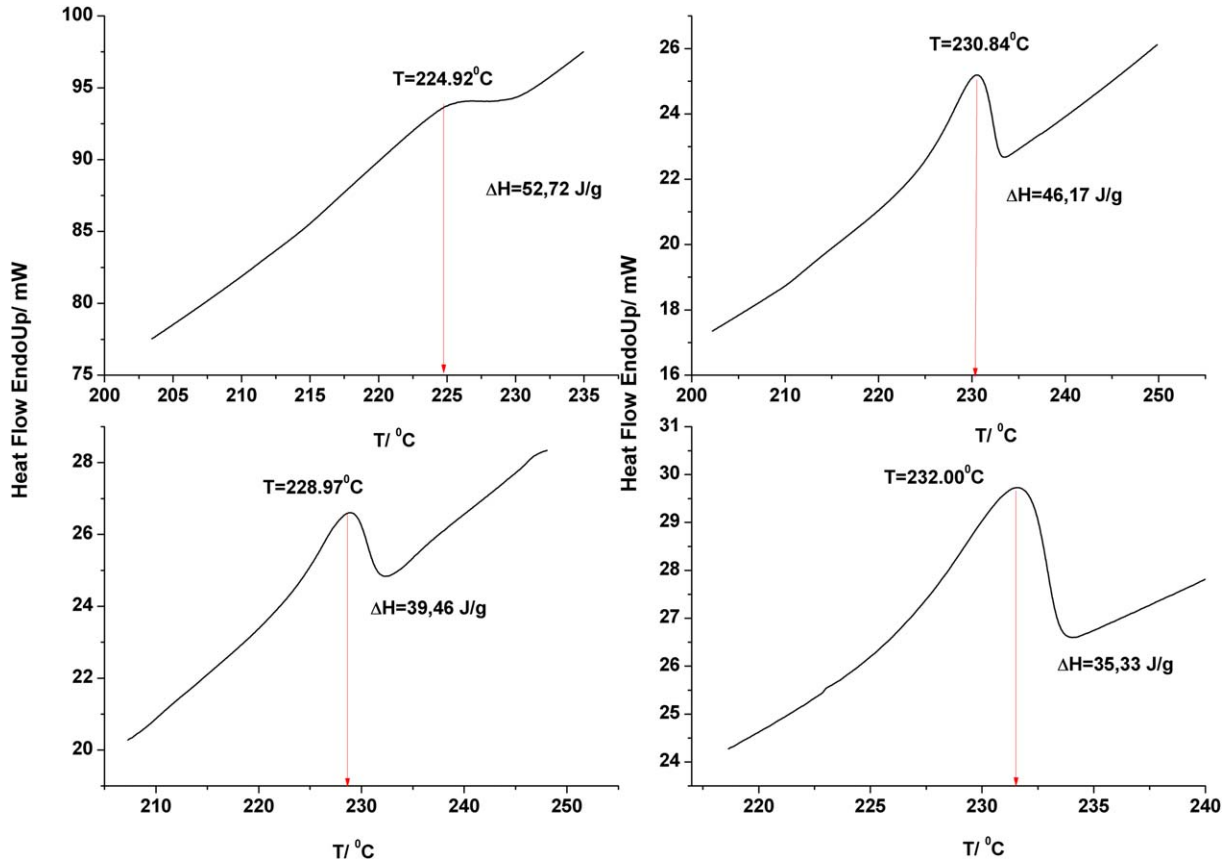

Figure 2. DSC thermograms. [Color figure can be viewed in the online issue, which is available at wileyonlinelibrary.com.]

suggests an increasing of the polymeric chains flexibility. The highest SD of PVA/Scl is in good accordance with this. On the contrary, the shift of the absorption band from 674.81 cm^{-1} to 680.16 cm^{-1} in case of PVA/zein suggests the increase of the PVA chains rigidity after zein blending and a lower SD for PVA/Zein cryogels. In case of PVA/Scl and PVA/Cel cryogel spectra, a new absorption band (at 2350 cm^{-1}) specific to acetals groups can be observed (most glycoside bonds in carbohydrates and other polysaccharides are acetal linkages, here Scl and Cel). As for the PVA/Cel spectra there is a cellulose specific band at 1725 cm^{-1} (corresponding to C═O stretching vibration found in cellulose spectra[27]). These new bands are suggesting the presence of Scl and Cel inside PVA cryogel without new covalent bonds forming.

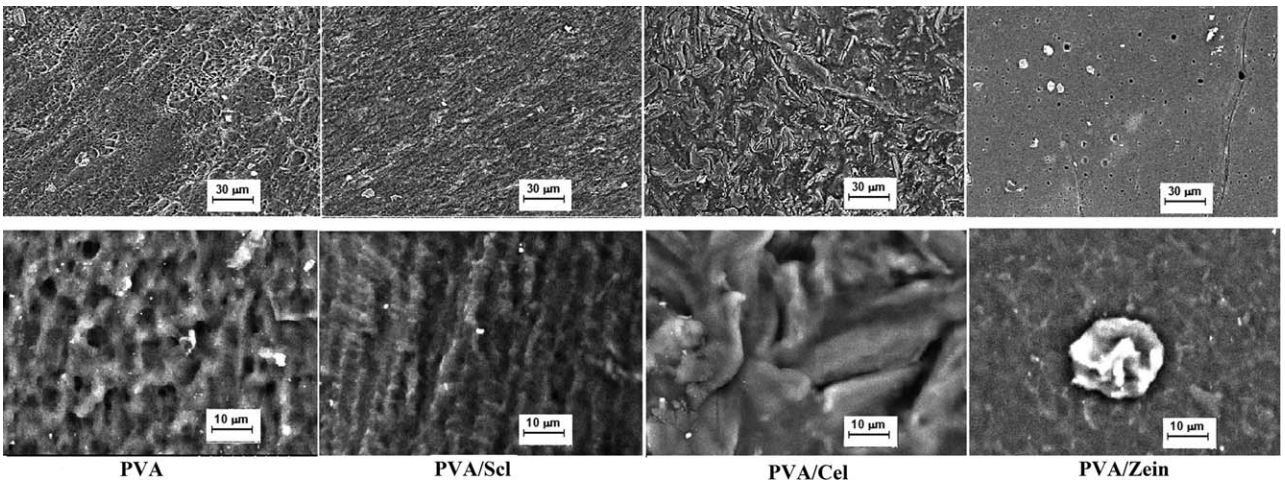

Figure 3. SEM images of PVA membranes (20 kV, Magnification 150×).

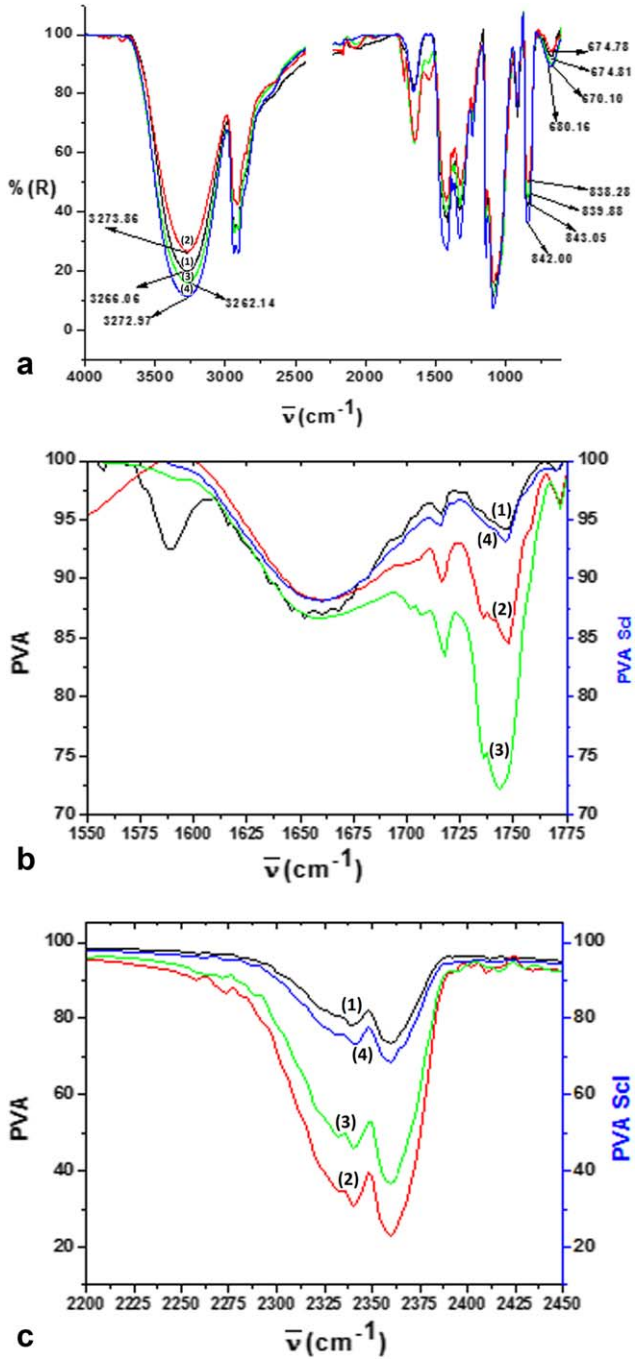

Figure 4. FTIR spectra for PVA and PVA/bioinsertions cryogels (**a**); detailed scale (**b**); detailed scale (**c**) ((3) green-PVA/Zein; (2) red-PVA/Scl; (1) black-PVA; (4) blue-PVA/Cel). [Color figure can be viewed in the online issue, which is available at wileyonlinelibrary.com.]

A complementary method (successfully used in our previous study of MB sorption on the same cryogelic membranes) and that gives important information concerning the gels morphology and dyes sorption capacity is the CIELAB analysis. Photographic images show that PVA/Scl cryogels have much more intense violet color compared with the other cryogels meaning, like in MB sorption case,[11] an increased sorption capacity of this gel (Figure 5). Comparing the mass of the sorbed dye after

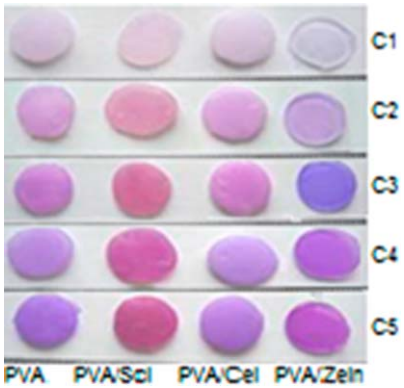

Figure 5. Images of PVA based cryogels after CV sorption. [Color figure can be viewed in the online issue, which is available at wileyonlinelibrary.com.]

equilibrium reaching for the two dyes, CV and MB, it can observed that, in both cases, the highest value was obtained for the PVA/Scl cryogels (for CV the sorbed mass is increasing from 0.338 to 3.388 mg/g for PVA/Scl as for MB is increasing from 1.949 to 9.528 mg/g), depending on each dye's initial concentration. In fact, the sorbed mass values for both dyes are following the same trend: PVA/Scl > PVA > PVA/Cel > PVA/Zein but the amount of CV sorbed in all cryogels is higher than in MB case, in the same concentration range.

From photographic images shown in Figure 5 it can be observed that PVA, PVA/Cel, and PVA/Zein cryogels have a blue-violet color while those of PVA/Scl is a pink-violet one. From the graphical representation of the parameter a^* against the initial immersion solutions concentrations [Figure 6(a)] it can be observed that this parameter increases (red component), meaning absorption of green color, in all cryogels and for all concentrations. This absorption of the green color in the visible range is a shift to lower wavelengths or a shift to blue (blue shift) and is correlated with the presence of dimers and molecular aggregates when the concentration of the dye increases.[28] In accordance with the literature data[27,29] for concentrations smaller than $5 \times 10^{-6} M$ (c_1–c_3), the dye cation is in the monomeric form CV^+, while the c_4–c_5 solutions contain the dye in the dimeric form.[30]

The small increase of $+a^*$ parameter (red color) for PVA/Cel cryogel comparing to the others [Figure 6(a)] may be due to a favorable orientation of CV^+ plan on the gel surface considering the presence of more ordered microcellulose formations contained in the cryogel. On the other hand, the pink-violet color of PVA/Scl cryogels is evidenced by the variation of the $-b^*$ parameter (blue color) and by the highest value for of the ratio between a^*/b^* parameters showed in Figure 6(c) (in fact the ratio between red and blue color). In MB sorption case, the possibility of dye penetration into Scl internal channel was excluded due to the MB molecule dimensions.[11] Taking into account the molecule surface area (MSA) for the MB (426.52 Å)[31] and for the CV (585.26 Å)[32] this possibility was also excluded.[33]

Furthermore, comparing the values for the difference in color (ΔE^*_{ab}) and the luminosity (ΔL^*) of samples after CV sorption (Figure 7) with those obtained after MB sorption[11] it can be

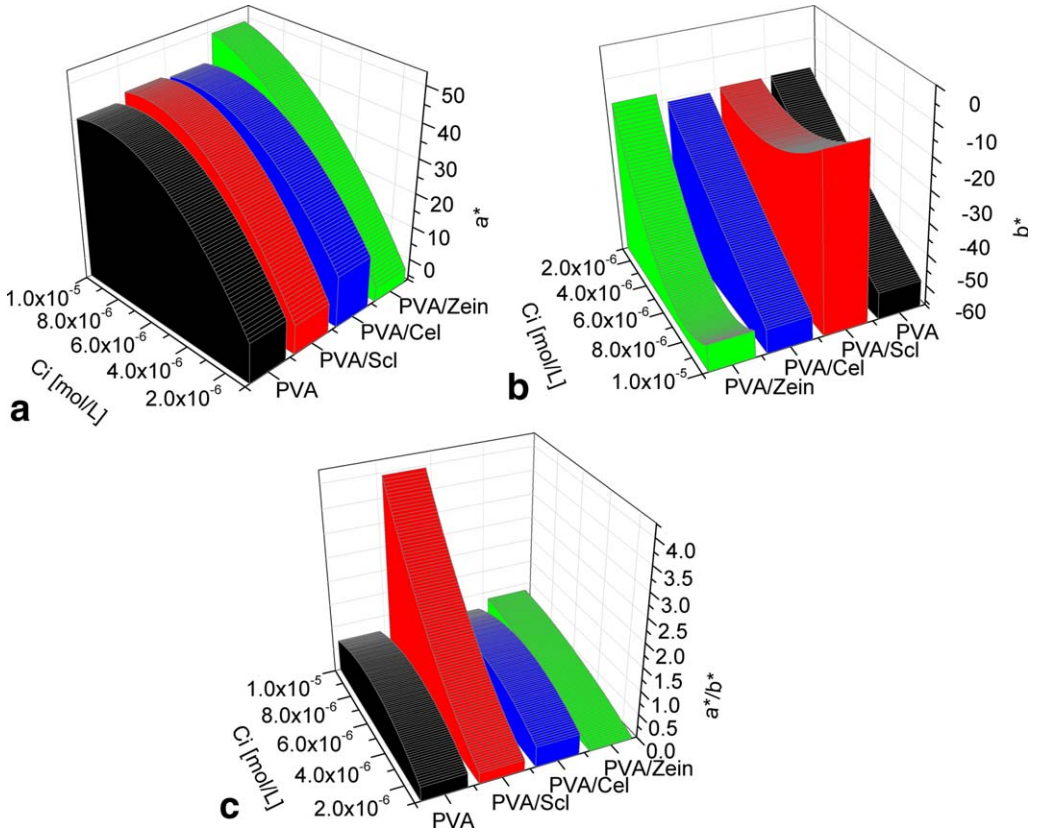

Figure 6. Variation of a^* (**a**), b^*parameter (**b**), and of their ratio, a^*/b^* (**c**) of cryogels. [Color figure can be viewed in the online issue, which is available at wileyonlinelibrary.com.]

observed that both of them are lower, in good agreement with the extinction coefficient, ε ($87.000M^{-1}$ cm^{-1} for CV[25] and $95.000M^{-1}$ cm^{-1}, for MB[34]). The difference in color (ΔE^*_{ab}) from Figure 7 shows the lowest values for PVA/Scl gels and the highest, for the PVA/Zein gels. These values are in good agreement with the fact that, the largest contact surface of the PVA/Scl gels, that are highly porous, determines a better dye dispersion in the whole mass of the gel and consequently, a lighter color, while the lowest contact surface for PVA/Zein gels, which are more compact, determines a maximum agglomeration of the dye at the gel's surface, equivalent with a higher dye concentration, and thus a darker color. As also observed in Figure 6, the samples luminosity for all cryogels is concentration dependent, decreasing with the concentration increase. The lowest luminosity values are, as expected, for the PVA/Scl gel, which has the highest amount of the sorbed dye and for the PVA/Zein gels, which has the most compact structure.

In conclusion, the analysis of the cryogels with the CIELAB system supports the data obtained for the amount of the sorbed

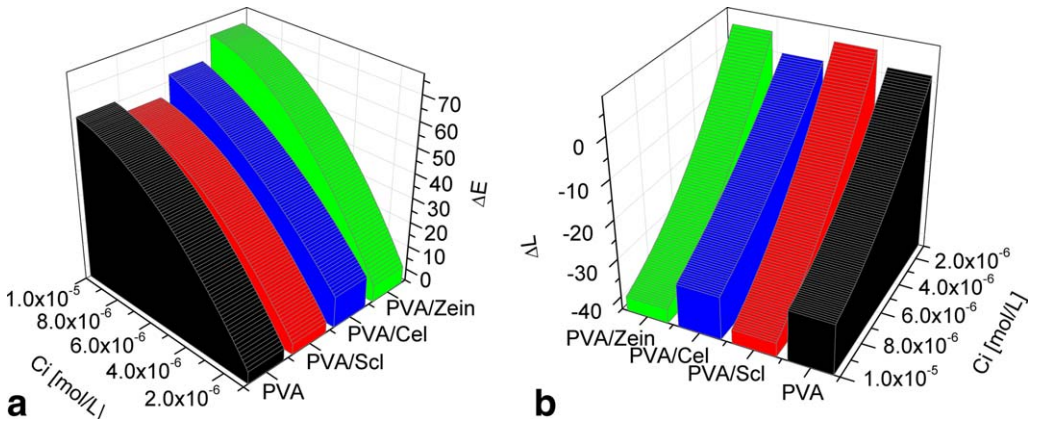

Figure 7. Variation of ΔE^* (**a**) and ΔL^* (**b**) parameters of cryogels. [Color figure can be viewed in the online issue, which is available at wileyonlinelibrary.com.]

Table II. CV Sorption Rate in Cryogels

Cryogel type	The initial concentration for CV (mol/L)				
	C_1 (1.00×10^{-6})	C_2 (3.00×10^{-6})	C_3 (5.00×10^{-6})	C_4 (7.00×10^{-6})	C_5 (1.00×10^{-5})
	The sorption rate $\times 10^4$ (mg/g min)				
PVA	0.988	4.961	6.496	9.060	11.150
PVA/Scl	1.608	4.077	11.755	8.566	18.455
PVA/Cel	0.994	3.299	4.465	6.868	6.968
PVA/Zein	0.948	2.733	4.729	6.441	10.096

dye into the cryogels (obtained through VIS analysis of solutions of gel's immersion) which shows that PVA/Scl cryogels remove the highest quantity of dye as a result of its special structure. The CV^+ sorption on the external and internal surface of gels is determined both by the dye–dye interaction and by the interaction of the free pairs of electrons of oxygen from the OH groups (present in all polymers) with π electrons of CV^+ (both monomer or dimer form).

In order to use these cryogels in the advanced wastewater purification process, the sorption rate was determined. It was found that dye accumulation in cryogels increases with the CV solutions concentration increase and with the period of immersion. Plotting solutions concentration variation against the time of immersion, the sorption rate can be calculated. It was found that the sorption rate is higher if the initial dye concentration is high (Table II) due to the high concentration gradient.

The sorption rate for CV was found to be until 2.3 times higher than sorption rate for MB in the same concentration range and for the same type of cryogels. Like in the MB sorption the results confirm a faster dye accumulation in PVA/Scl than in the other cryogels. The adsorption kinetic at the solid-phase interface was studied to determine the uptake rate of the dye. Experimental data were analyzed using: the pseudo-first-order kinetic model, the pseudo-second-order kinetic model and Weber–Morris intra-particle diffusion model.

The differential and linear forms of pseudo-first-order kinetic model are given as:[35]

$$\frac{dq_t}{dt} = k_1(q_e - q_t) \tag{8}$$

$$\log(q_e - q_t) = \log q_e - \frac{k_1}{2.303}t \tag{9}$$

where, q_e is the amount of dye sorbed at equilibrium (mg/g); q_t is the amount of dye sorbed at time t (mg/g); k_1 is the equilibrium rate constant of pseudo-first sorption (min^{-1}).

Plotting $\log(q_e - q_t)$ versus t, the sorption rate constant, k_1, and the correlation coefficient, R^2_1 were calculated. The values for R^2_1 in the range of 0.7291–0.9453 suggest that the sorption process does not follow the pseudo-first-order sorption rate expression of Lagergren. For that reason, the pseudo-second-order equation was further used[11] where, k_2 is the rate constant of sorption, q_t and q_e are the amount sorbed at time t and, respectively, at equilibrium (in mg/g).

$$\frac{t}{q_t} = \frac{1}{h} + \frac{1}{q_e}t \tag{10}$$

Therefore from the slope and, respectively, the intercept of plot t/q_t versus t, the rate constant k_2, initial sorption rate h, and predicted q_e can be calculated.[35]

Weber–Morris intra-particle diffusion model has also been used to determine CV sorption rate in the membranes. The amount adsorbed is given by eq. (11):[36–38]

$$q_t = k_{id} \times t^{1/2} + f_i \tag{11}$$

where, k_{id} [mg/(g $min^{1/2}$)] is the intra-particle diffusion rate constant obtained from the slope of the straight line of q_t versus $t^{1/2}$, as shown in Figure 8 and f_i which is a constant and the value of intercept. If the plot satisfies the linear relationship with the experimental data, then the sorption process is found to be controlled by intra-particle diffusion only. The adsorption in this model involves two steps: (1) surface diffusion and (2) intra-particle diffusion and does not satisfies the linear relationship, meaning that the diffusion process is not controlled by intra-particle diffusion (Figure 8).

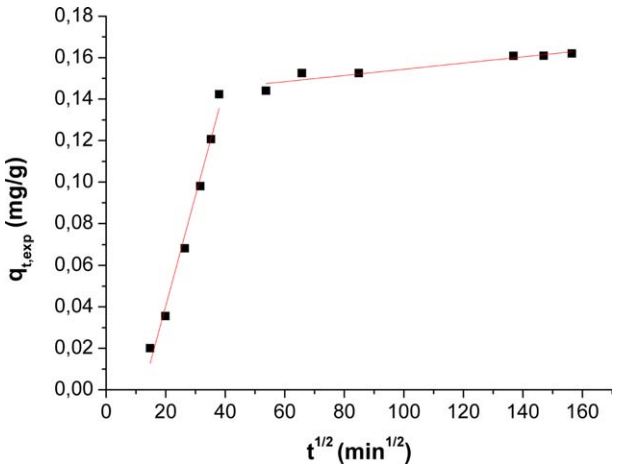

Figure 8. Graphical representation of Weber–Morris intra-particle diffusion model for CV (c_1 concentration) sorption in PVA cryogel. [Color figure can be viewed in the online issue, which is available at wileyonlinelibrary.com.]

The obtained values for the kinetic parameters (for pseudo-first, pseudo-second-order equations, and intra-particle diffusion model) together with the correlation coefficients and values of the obtained experimental data (q_e exp) are given in Tables III–VI.

The R^2_2 values lies between 0.9955 and 0.9989 showing good linearity. Comparing the values for the initial sorption rate h for CV with the same values obtained for MB, in the same concentration range, it was noticed that they are lower for the PVA/Scl (1.93 mg/g min < 15.19 mg/g min) and PVA/Zein gels (1.203 mg/g min < 5.58 mg/g min) and higher for the PVA (20.08 mg/g min > 8.47 mg/g min) and PVA/Cel gels (13.13 mg/g min > 6.07 mg/g min). It was also observed that if the initial concentration of dye is increasing the initial sorption rate and the equilibrium sorption capacity are also increasing, whereas pseudo-second-order-rate constant k_2 is generally, decreasing (the lowest values of k_2 were obtained for PVA/Scl). Taking into consideration that k_2 decreases faster in the lower concentration domain (2×10^{-6} to 3×10^{-6} mol/L) it can conclude that these cryogels are efficient in removal of the CV dye from diluted solutions. From intra-particle model results, it can be seen that with CV concentration increase, the line slope increases, showing that CV surface adsorption is increasing (many of the CV molecules are interacting with active sites on adsorbent). When all of the exterior active sites were occupied, CV molecules seek to enter into the pores of the adsorbents corresponding to the second linear portion of the curves, and determining the intra-particle diffusion. Moreover, the diffusion rate constants for all membranes in all concentrations follow the order of: $k_{i,1} > k_{i,2}$ (Tables III–VI) showing that the first diffusion stage is the fastest. According to the results, the intra-particle diffusion model shows a poor fit to the experimental data in comparing to the pseudo-second-order model that has the highest conformity with the experimental data.

The equations that correlate the parameters q_e with the initial concentration (c_0) of CV in aqueous solution have been determined and are presented in Table VII. In this way, the pseudo-second-order kinetic expressions were tested for its consistency in predicting the amount of CV adsorbed for the entire sorption domain like in previous study for MB[11] but the correlation coefficients in this case are higher showing a better fitting. Applying the calculated kinetic constants, the q_t values were predicted. The pseudo-second-order kinetic expression can be obtained by substituting the k_2 and predicted q_e values in eq. (12):

$$q_t = \frac{t}{\frac{1}{k_2 q_e^2} + \frac{t}{q_e}} \tag{12}$$

The q_t values predicted by the kinetic model were compared with the amount of the sorbed CV obtained experimentally. It was observed that for the entire studied sorption period, the predicted sorbed amount (q_t) of CV is in agreement with the experimental data (q_{exp}). This agreement suggests that the Ho pseudo-second-order kinetic model can be applied to predict the amount of CV uptake at different contact time intervals and at equilibrium state. Similar results were obtained by other researchers for the CV sorption on palm kernel fibers.[39]

Table III. Kinetic Parameters for CV Adsorption in PVA Cryogels

	Pseudo-first-order equation			Pseudo-second-order equation				W–M intra-particle diffusion model				
$C_0 \times 10^6$ (mol/L)	$k_1 \times 10^4$ (g/(mg min))	$q_{e,predicted}$ (mg/g)	R_1^2	$k_2 \times 10^4$ (g/(mg min))	$h \times 10^4$ (mg/(g min))	$q_{e,predicted}$ (mg/g)	$q_{e,exp}$ (mg/g)	R_2^2	$k_{i,1}$ (mg/(g min$^{1/2}$))	f_1 (mg/g)	R^2	$k_{i,2}$ (mg/(g min$^{1/2}$))	f_2 (mg/g)	R^2
1.00	3.526	0.0898	0.7291	72.988	2.057	0.1678	0.1592	0.9978	0.0053	0.0653	0.9818	0.00015	0.13941	0.8759
3.00	3.405	0.6053	0.7736	1.702	9.288	0.8909	0.8717	0.9955	0.0264	0.3159	0.9873	0.00055	0.71968	0.8863
5.00	1.158	0.5355	0.8280	8.673	1.284	1.1900	1.1863	0.9986	0.0335	0.3842	0.9794	0.00175	0.87970	0.9979
7.00	1.315	0.5259	0.7807	8.736	20.088	1.5163	1.5000	0.9982	0.0485	0.5848	0.9832	0.00143	1.24918	0.9525
10.0	1.186	0.8229	0.7363	5.402	22.705	2.0501	2.0381	0.9980	0.0580	0.6886	0.9676	0.00158	1.72624	0.9514

Table IV. Kinetic Parameters for CV Adsorption in PVA/Scl Cryogels

Pseudo-first-order equation				Pseudo-second-order equation					W-M intra-particle diffusion model					
$C_0 \times 10^6$ (mol/L)	$k_1 \times 10^4$ (g/(mg min))	$q_{e,predicted}$ (mg/g)	R_1^2	$k_2 \times 10^4$ (g/(mg min))	$h \times 10^4$ (mg/(g min))	$q_{e,predicted}$ (mg/g)	$q_{e,exp}$ (mg/g)	R_2^2	$k_{i,1}$ (mg/(g $min^{1/2}$))	f_1 (mg/g)	R^2	$k_{i,2}$ (mg/(g $min^{1/2}$))	f_2 (mg/g)	R^2
1.00	2.189	0.1991	0.8817	22.252	2.780	0.3534	0.3375	0.9977	0.0054	0.0215	0.9016	0.00046	0.26480	0.9500
3.00	1.490	0.5993	0.8994	5.534	6.804	1.1088	1.0536	0.9971	0.0168	0.1310	0.9521	0.00104	0.87212	0.9862
5.00	1.252	0.7511	0.7326	5.919	2.552	2.0365	2.0192	0.9975	0.0657	0.8602	0.9918	0.00162	1.71724	0.8559
7.00	1.779	1.4232	0.9453	2.171	1.930	2.5328	2.3597	0.9973	0.0382	0.3553	0.9718	0.00308	1.86915	0.9833
10.0	1.306	1.5238	0.8553	2.998	35.260	3.4295	3.3882	0.9983	0.1002	1.2688	0.9788	0.00488	2.55558	0.9952

Table V. Kinetic Parameters for CV Adsorption in PVA/Cel Cryogels

Pseudo-first-order equation				Pseudo-second-order equation					W-M intra-particle diffusion model					
$C_0 \times 10^6$ (mol/L)	$k_1 \times 10^4$ (g/(mg min))	$q_{e,predicted}$ (mg/g)	R_1^2	$k_2 \times 10^4$ (g/(mg min))	$h \times 10^4$ (mg/(g min))	$q_{e,predicted}$ (mg/g)	$q_{e,exp}$ (mg/g)	R_2^2	$k_{i,1}$ mg/(g $min^{1/2}$)	f_1 (mg/g)	R^2	$k_{i,2}$ (mg/(g $min^{1/2}$))	f_2 (mg/g)	R^2
1.00	1.922	0.0558	0.8346	85.406	2.4057	0.1678	0.1634	0.9986	0.0053	0.0641	0.9814	0.00009	0.14957	0.9228
3.00	1.201	0.2299	0.7844	20.349	7.0751	0.5896	0.5874	0.9981	0.0181	0.2290	0.9881	0.00062	0.47586	0.9376
5.00	1.512	0.3166	0.8646	15.414	10.092	0.8091	0.7943	0.9989	0.0234	0.2714	0.9816	0.00090	0.64496	0.9280
7.00	1.293	0.5277	0.8373	8.000	13.129	1.2501	1.2335	0.9977	0.0385	0.4972	0.9939	0.00158	0.96070	0.9827
10.0	1.878	0.5660	0.7776	8.327	13.452	1.2709	1.2388	0.9973	0.0385	0.5023	0.9876	0.00119	1.03730	0.9561

Table VI. Kinetic Parameters for CV Adsorption in PVA/Zein Cryogels

	Pseudo-first-order equation			Pseudo-second-order equation				W–M intra-particle diffusion model					
$C_0 \times 10^6$ (mol/L)	$k_1 \times 10^4$ (g/mg min))	$q_{e,predicted}$ (mg/g)	R_1^2	$k_2 \times 10^4$ (g/(mg min))	$h \times 10^4$ (mg/(g min))	$q_{e,predicted}$ (mg/g)	$q_{e,exp}$ (mg/g)	R_2^2	$k_{i,1}$ (mg/(g $min^{1/2}$))	f_1 (mg/g)	R^2	$k_{i,2}$ (mg/(g $min^{1/2}$))	f_2 (mg/g)	R^2
1.00	2.378	0.0703	0.9162	69.027	1.902	0.1660	0.1596	0.9988	0.0033	0.0215	0.9749	0.00011	0.14323	0.8153
3.00	2.784	0.2616	0.8974	20.315	5.507	0.5206	0.4989	0.9981	0.0108	0.0836	0.9204	0.00040	0.43815	0.9939
5.00	1.756	0.3713	0.8046	12.168	9.272	0.8729	0.8485	0.9969	0.0270	0.3609	0.9866	0.00100	0.68177	0.8618
7.00	1.550	0.4357	0.7195	9.348	1.203	1.1884	1.1641	0.9965	0.0366	0.4987	0.9879	0.00018	1.08750	0.8210
10.0	1.566	0.7088	0.8367	6.275	2.181	1.7933	1.7506	0.9980	0.0546	0.7098	0.9880	0.00126	1.50400	0.9790

Table VII. The Expressions q_e as Function of c_0

Cryogel type	Expression of q_e as function of c_o	R^2
PVA	$q_e = 0.133 + 198,095.835c_0$	0.9582
PVA/Scl	$q_e = 0.114 + 342,004.212c_0$	0.9843
PVA/Cel	$q_e = 0.158 + 126,781.788c_0$	0.8732
PVA/Zein	$q_e = 0.022 + 17,889.203c_0$	0.9978

To describe the interactions between the molecules of adsorbate and the adsorbent surface, adsorption isotherms were studied. Like previously[11] most widely used isotherm models (Langmuir and Freundlich) were tested. As in the MB adsorption case, the result shows that Freundlich isotherm best-fit the equilibrium data for adsorption of CV. The Freundlich isotherm model is considered to be appropriate for describing both multilayer sorption and sorption on heterogeneous surfaces[40] and is expressed by eq. (13):

$$q_e = K_F c_e^{1/n} \tag{13}$$

where: K_F is the Freundlich constant (a measure which shows the strength of the interaction between adsorbate and adsorbent) and $1/n$ is the adsorption intensity whose values show the type of adsorption: irreversible for $1/n = 0$, favorable for $0 < 1/n < 1$ and unfavorable for $1/n > 1$. K_F and $(1/n)$ can be determined from the linear plot of log q_e versus log c_i or log c_e.[11,40] In agreement with the literature data[40] the isotherms have been modeled both as a function of c_e and as a function of c_i and these two types of isotherms were analyzed and compared (Table VIII).

From Table VIII, no significant differences between the correlation coefficients for the two models (using c_e or c_i) are shown but using c_i is easier and more favorable in order to compare the effectiveness of different sorbents. Furthermore, using c_i, higher values of both K_F and $1/n$ were obtained, indicating a higher uptake of the dye. The values of the Freundlich exponents are higher than the same values obtained for MB in the same concentration range, and like in previous case, they are in the range of $0 < 1/n < 1$, showing favorable sorption condition.

In addition to CV sorption study, the transport of CV through the modified membranes was monitored. So, using a diffusion cell, the permeability of the PVA with bioinsertion cryogels for CV was tested. After that, diffusion (D) and permittivity (P) coefficients were calculated and they are presented in Table IX. Generally, the membrane permeability is determined by the amorphous part and not by crystalline one,[23] but it is possible that an increase of the CD of the membrane to increase the P coefficient. This could happen because OH groups from the PVA molecules are bonded through hydrogen bonds in crystallites and they cannot interact with CV molecules, which can diffuse through pores. Here, the decrease of the P coefficient (in case of bioinsertion/PVA membranes comparing to PVA membrane) can be attributed to the pores decrease as it can be seen from SEM pictures (Figure 2). The diffusion coefficient is also decreasing in all cases comparing to D_{PVA}. Generally, with steady-state transport processes through membranes, there is a time-lag (θ) associated with the dissolution of the permeant

Table VIII. Freundlich Isotherm Parameters for Adsorption Data Plotted in Terms of the CV's Initial Concentration (c_i) and Equilibrium Concentration (c_e) in Solutions

	$q_e = f(c_i)$			$q_e = f(c_e)$		
Cryogel type	K_F (mg/g)(L/mol)$^{1/n}$	$1/n$	R^2	K_F (mg/g)(L/mol)$^{1/n}$	$1/n$	R^2
PVA	153175.745	1.0141	0.9599	25025.341	0.7834	0.9630
PVA/Scl	91839.603	0.9303	0.9894	195330.472	0.8847	0.8873
PVA/Cel	15510.293	0.8464	0.9618	3655.443	0.6559	0.9575
PVA/Zein	56781.910	0.9525	0.9985	6644.006	0.6679	0.9952

species until equilibrium is achieved. In addition, an increase in the induction period may be found with an increase in the interaction between the permeant species and the polymeric matrix.[41] The permeation of CV from 0.1 m*M* initial solution, through PVA membranes leads to a time lag varying from 9 to 13.5 h followed by a steady-state flux. Time-lag values are increasing in all cases comparing to PVA not only because of the membrane compaction and closes of the pores but also because of the interactions between polymer and every bioinsertion. It was found that the integral diffusion coefficient of CV, as calculated by eq. (6), depends of membrane thickness (the diffusion coefficient increases with the membrane thickness). The distribution coefficient obtained by the time-lag technique, K_θ, defined as P/D_θ, gives a value of $K_\theta = 23.23$ for PVA, indicating that the PVA matrix has a great affinity to CV dye but smaller then PVA/Scl and PVA/Zein. In PVA/Cel case the affinity to CV is lower than the PVA matrix, which is in close agreement with sorption rates (the membrane with Cel having the lowest sorption rate for high concentrations, see the value for c_5 in Table II).

Kinetic and thermodynamic results show a good accordance with the spectroscopic analysis and they are complementary with the CIELAB results for gels color analysis. The color changes of the loaded cryogels suggest the association and different distribution types of the dye in the gel, like in previous MB study; the presence of dimers and molecular aggregates is associated with the increases of dye concentration. All the methods of study have emphasized that the tested gels have the ability to adsorb the dye from aqueous solutions but the best sorption properties have been proved by the PVA/Scl cryogels. PVA/Cel and PVA/Zein cryogels have a lower capacity of dyes retention but they are mechanically stronger. By comparing the results obtained in this study with those reported in other studies[11,15,42] it can be concluded that the prepared gels favor the simultaneous sorption of dyes from aqueous solutions but the sorbed amount depends beside the dye initial concentration and dye solubility, on the type of bioinsertions. The last ones influence both the cryogel morphology and the type of interaction with dye molecules.

Table IX. Diffusion (D) and Permittivity (P) Coefficients of CV Through PVA, PVA/Scl, PVA/Cel, and PVA/Zein Membranes

Membrane type	t_m (cm)	$P \times 10^6$ (cm^2 s^{-1})	$D_\theta \times 10^6$ (cm^2 s^{-1})	θ (h)	$K_\theta = P/D$
PVA	0.212	5.46	2.35	9	23.23
PVA/Scl	0.170	4.86	1.33	10	36.52
PVA/Cel	0.228	4.15	2.21	11	18.73
PVA/Zein	0.154	2.57	0.81	13.5	31.56

CONCLUSIONS

The study evidenced that the bioinsertions change the PVA cryogel morphology by alteration of the PVA crystallinity, porosity and thus, by modifying of the contact surface of the gel. Consequently, the type of biopolymer determines the amount of the sorbed dye and the sorption kinetics. Also, the PVA cryogel color changes with bioinsertion type making possible its use in colored fibers obtaining.

In addition, the comparison between the sorption rates of both studied dyes (MB and CV) shows higher values for CV, information which is very useful when the two dyes have to be simultaneously removed from aqueous solutions (application: in wastewater purification).

Nevertheless diffusion experiments confirm that addition of bioinsertions to PVA will increase interactions between the cryogel and the dye (showed also by CIELAB analysis) by showing lower values for the P and D coefficients by comparing to PVA.

ACKNOWLEDGMENTS

This article was supported by the Sectoral Operational Programme Human Resources Development (SOP HRD), financed from the European Social Fund and by the Romanian Government under the project number POSDRU/159/1.5/S/134378.

REFERENCES

1. Li, X.; Li, Y.; Zhang, S.; Ye, Z. *Chem. Eng. J.* **2012**, *183*, 88.
2. Sandeman, S. R.; Gun'ko, V. M.; Bakalinska, O. M.; Howell, C. A.; Zheng, Y.; Kartel, M. T.; Phillips, G. J.; Mikhalovsky, S. V. *J. Colloid Interf. Sci.* **2011**, *358*, 582.
3. Liu, Y.; Zheng, Y.; Wang, A. *J. Environ. Sci.* **2010**, *22*, 486.
4. Sanghi, R.; Bhattacharya, B. *Color. Technol.* **2002**, *118*, 256.
5. Vilar, V. J. P.; Botelho, C. M. S.; Boaventura, R. A. R. *J. Hazard Mater.* **2007**, *147*, 120.
6. Crini, G.; Badot, P. M. *Prog. Polym. Sci.* **2008**, *33*, 399.

7. Deligkaris, K.; Shiferaw Tadele, T.; Olthuis, W.; van den Berg, A. *Sensor Actuat. B* **2010**, *147*, 765.
8. Tran, T.; Hoang, M.; Xie, Z.; Bolto, B. *Prog. Polym. Sci.* **2009**, *34*, 969.
9. Hassan, C. M.; Peppas, N. A. *J. Appl. Polym. Sci.* **2000**, *76*, 2075.
10. Paduraru, O. M.; Vasile, C.; Patachia, S.; Grigoras, C.; Oprea, A. M. *Polimery* **2010**, *55*, 473.
11. Dobritoiu, R.; Patachia, S. *Appl. Surf. Sci.* **2013**, *285P*, 56.
12. Papancea, A.; Valente, A. J. M.; Patachia, S. *J. Appl. Polym. Sci.* **2010**, *118*, 1567.
13. Papancea, A.; Valente, A. J. M.; Patachia, S. *J. Appl. Polym. Sci.* **2010**, *115*, 1445.
14. Patachia, S.; Friedrich, Chr.; Florea, C.; Thomann, Y. *Express Polym. Lett.* **2011**, *5*, 197.
15. Patachia, S.; Damian, L. *Soft Mater.* **2014**, *12*, 371.
16. Survase, S. A.; Saudagar, P. S.; Bajaj, I. B.; Singhal, R. S. *Food Technol. Biotechnol.* **2007**, *45*, 107.
17. El-Sakhawy, M.; Hassan, M. L. *Carbohydr. Polym.* **2007**, *67*, 1.
18. Mathew, A. P.; Oksma, K.; Sain, M. *J. Appl. Polym. Sci.* **2005**, *97*, 2014.
19. Torres-Ginera, S.; Gimenezb, E.; Lagarona, J. M. *Food Hydrocoll.* **2008**, *22*, 601.
20. Kim, J.; Montero, G.; Habibi, Y.; Hinestroza, J. P.; Genzer, J.; Argyropoulos, D. S.; Rojas, O. *J. Polym. Eng. Sci.* **2009**, *49*, 2054.
21. Ahmad, R. *J. Hazard. Mater.* **2009**, *171*, 767.
22. Fu, J.; Qiao, J.; Wang, X.; Ma, J.; Okada, T. *Synth. Metals* **2010**, *160*, 193.
23. Sperling, L. H. Introduction to Physical Polymer Science, 3rd ed.; Wiley-Interscience: New York, **2001**.
24. Peppas, N. A.; Hansen, P. J. *J. Appl. Polym. Sci.* **1982**, *27*, 4787.
25. Cenens, J.; Schoonheydt, R. A. *Clays Clay Miner.* **1988**, *36*(3), 214.
26. Patachia, S.; Valente, A. J. M.; Baciu, C. *Eur. Polym. J.* **2007**, *43*, 460.
27. Gyu, B.; Jung, R. S.; Kim, K. *J. Bull. Korean Chem. Soc.* **1989**, *10*, 148.
28. Ibrahim, M. M.; El-Zawawy, W. K.; Nassar, M. A. *Carbohydr. Polym.* **2010**, *79*, 694.
29. http://en.wikipedia.org/wiki/Ionic_radius (accessed March 16, 2014).
30. Stork, W. H. J.; Lippits, G. J. M.; Mandel, M. *J. Phys. Chem.* **1972**, *76*, 1772.
31. Hang, P. T.; Brindley, G. W. *Clays Clay Miner.* **1970**, *18*, 203.
32. .http://www.chemicalize.org/structure (accessed May 20, 2014).
33. Wang, L.; Wang, A. *Bioresour. Technol.* **2008**, *99*, 1403.
34. Adams, E. Q.; Rosenstein, L. *J. Am. Chem. Soc.* **1914**, *36*(7), 1452.
35. Ho, Y. S.; McKay, G. *Trans. IchemE* **1998**, *76B*, 332.
36. Tanhaei, B.; Ayati, A.; Lahtinen, M.; Sillanpää, M. *Chem. Eng. J.* **2015**, *259*, 1.
37. Masoumi, A.; Ghaemy, M. *Carbohydr. Polym.* **2014**, *108*, 206.
38. Mane, V. S.; Vijay Babu, P. V. *J. Taiwan Inst. Chem. Eng.* **2013**, *44*, 81.
39. Owes El-Sayed, G. *Desalin.* **2011**, *272*, 225.
40. Coles, C. A.; Yong, R. N. *Eng. Geol.* **2006**, *85*, 19.
41. Hansen, C. M. Surface Effects Versus Bulk Phenomena as Explanations of Anomalous Absorption in Polymers. www.hansen-solubility.com (accessed March 20, 2014).
42. Patachia, S.; Dobritoiu, R.; Coviello, T. *Environ. Eng. Manag. J.* **2011**, *10*, 193.